AUTHOR(S):

Ohsaki, Makoto; Hayakawa, Kentaro

NON-PARAMETRIC SHAPE DESIGN OF FREE-FORM SHELLS USING FAIRNESS MEASURES AND DISCRETE DIFFERENTIAL GEOMETRY

Makoto OHSAKI[1] and Kentaro HAYAKAWA[2]

[1]Dr. Eng., Dept. of Architecture and Architectural Engineering, Kyoto University,
Kyoto-Daigaku Katsura, Nishikyo, Kyoto 615-8540, Japan,
ohsaki@archi.kyoto-u.ac.jp

[2]M. Eng., Dept. of Architecture and Architectural Engineering, Kyoto University,
se.hayakawa@archi.kyoto-u.ac.jp

ABSTRACT

A non-parametric approach is proposed for shape design of free-form shells discretized into triangular mesh. The discretized forms of curvatures are used for computing the fairness measures of the surface. The measures are defined as the area of the offset surface and the generalized form of the Gauss map. Gaussian curvature and mean curvature are computed using the angle defect and the cotangent formula, respectively, defined in the field of discrete differential geometry. Optimization problems are formulated for minimizing various fairness measures for shells with specified boundary conditions. A piecewise developable surface can be obtained without a priori assignment of the internal boundary. Effectiveness of the proposed method for generating various surface shapes is demonstrated in the numerical examples.

Keywords: form-finding, shell, shape optimization, differential geometry, fairness measure, Gauss map

1. INTRODUCTION

In the process of designing free-form shells for roof structures [1], parametric surfaces such as non-uniform rational B-splines (NURBS) [2] are often used. For the design of various types of shell and membrane surfaces, optimization problems are often solved for maximizing the structural stiffness or minimizing the error from the desired target shape such as minimal surface, which is equivalent to the uniform tension surface, and developable surface, which can be developed (flattened or unfolded) to a plane without in-plane stretching or shearing deformation [3]. In the optimization process using parametric surfaces, the locations of control points are chosen as design variables. A piecewise developable surface can be modeled and optimized using the (1,*n*)-Bézier surface [4, 5]. However, discretization into triangular or quadrilateral mesh is needed for the evaluation of structural properties using finite element analysis. One solution to bridge the gap between shape modeling and structural analysis is to use isogeometric analysis [6]. Another approach is to directly design the discrete surface (polyhedral surface) that can be consistently used for structural design, analysis, and manufacturing. In this study, we use the latter approach and present a shape design method based on the discrete differential geometry [7].

Shape design of shell roof structures may be one of a few fields where collaboration between architects and engineers plays a key role in generating an aesthetically pleasing shape that is also mechanically efficient, where various metrics of fairness of the surfaces can be used [8]. The first author proposed a shape design method of arches and ribbed shells using the roundness metrics [9]. A method utilizing various geometrical invariants has also been proposed for designing local shapes of shells [10]. The constructability of the free-form shells can be significantly improved utilizing the theories and

93

methodologies of discrete differential geometry. Mesnil et al. [11] proposed Marionette mesh for designing a surface as an assembly of quadrilateral plates. Pinkall and Polthier [12] developed a method for generating discretized minimal surfaces. However, it is difficult to model a complex surface using a quadrilateral mesh. Hayashi et al. [13] proposed an approach to the design of piecewise convex surfaces with a triangular mesh based on the Gaussian curvature flow as a gradient flow of a special form of the energy functional of the linear Weingarten surface [14]. Shimoda and Yamane [15] utilized the discrete form of mean curvature for shape optimization of the membrane surface.

Stein et al. [16] proposed a method for generating piecewise developable discrete surfaces using the Gauss map generated from the unit normal vectors of triangular faces. The special cases where the Gauss map degenerates into a line or a point are discussed in detail, and a method is presented for minimizing an energy function to achieve a Gauss map such that the minimum width is zero except at the internal boundaries. In their method, the locations of internal boundaries need not be specified *a priori*; however, special care should be made for preventing a pathological case such as corrugated surfaces with spikes.

In this study, a non-parametric approach is proposed for shape design of free-form shells discretized into triangular mesh. The discretized forms of the normal vector, Gaussian curvature, and mean curvature are used for computing the fairness measures of the surface, which are defined as the areas of derived surfaces including the generalized forms of offset surface and Gauss map. The Gaussian curvature and the mean curvature are computed using the angle defect and the cotangent formula, respectively [12, 17, 18]. Optimization problems are formulated for minimizing various fairness measures of surfaces with specified boundary conditions. Using the proposed method, various piecewise developable surfaces can be generated for the specified boundary without specifying the locations of internal boundaries. The dependence of the shape on the mesh divisions is discussed. The edge lengths and the areas of the side faces of the triangular prism are also considered as the measure of fairness. Round shapes are also generated by minimizing the areas of the offset surfaces.

2. DISCRETIZED FORMS OF FAIRNESS MEASURES

Consider a process of designing a *primary* surface or *design* surface using the properties of a *derived* surface defined using the geometrical invariants of the primary surface. Suppose the primary surface $\mathbf{r}(s,t)$ is defined by the parameters (s,t). For a graph surface on the (x, y)-plane, the vertical z-coordinate is a function of (x, y)-coordinates in the horizontal plane as $z(x, y)$.

The generalized forms of offset surface and Gauss map are defined in the following unified form:

$$\mathbf{c}(s,t) = e\mathbf{r}(s,t) + f(s,t)\mathbf{n}(s,t) \qquad (1)$$

where $\mathbf{n}(s,t)$ is the unit normal vector, $e \in \{0,1\}$ is a parameter, and $f(s,t)$ is a function of geometrical invariants such as the Gaussian curvature and the mean curvature of the primary surface. The surface becomes an offset surface if $e = 1$, and the Gauss map $\mathbf{c}(s,t) = \mathbf{n}(s,t)$ is generated if $e = 0$ and $f(s,t) = 1$. Examples of an offset surface and a Gauss map are illustrated in Fig. 1. Various surfaces are generated by minimizing the area of $\mathbf{c}(s,t)$ as a fairness measure μ as

$$\mu = \int g(s,t)dsdt \qquad (2)$$

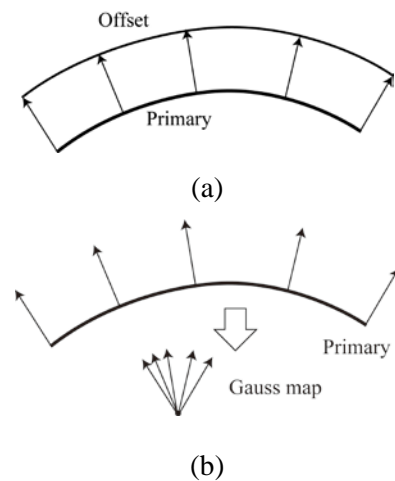where $g(s,t)$ is the determinant of the first fundamental form of the derived surface.

(a)

(b)

Figure 1: Examples of derived surface;
(a) offset surface, (b) Gauss map

Roulier and Rando [8] modeled the primary surface using a parametric form, and obtained the curvatures analytically; however, the analytical expression of

the integrant of the fairness measure in Eq. (2) is very complex. Since the integration in Eq. (2) is carried out discretely using numerical integration, it is preferable to compute the geometrical properties also in a discrete manner.

In the numerical examples, we consider the following four derived surfaces.

Case 1: $\mathbf{c}_1 = \mathbf{n}$,   Case 2: $\mathbf{c}_2 = (K + H^2)\mathbf{n}$,

Case 3: $\mathbf{c}_3 = \mathbf{r} - a\mathbf{n}$,   Case 4: $\mathbf{c}_4 = \mathbf{r} + \dfrac{H}{K}\mathbf{n}$

Note that $\mathbf{c}_1$ is the Gauss map, and $\mathbf{c}_2$ is a generalized form of Gauss map that is proposed as a rolling metric in Ref. [8]. The surfaces $\mathbf{c}_3$ and $\mathbf{c}_4$ are offset surfaces. The area of $\mathbf{c}_3$ vanishes if $\mathbf{r}$ is a sphere with the radius a. The area of $\mathbf{c}_4$ is proposed as a rounding metric in Ref. [8].

(a)

(b)
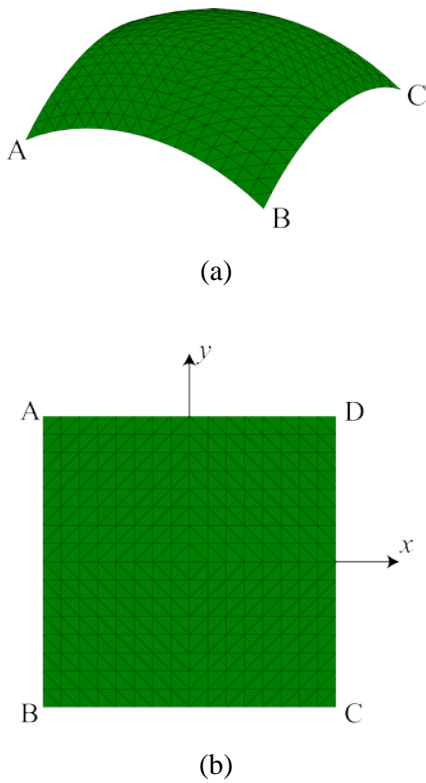
Figure 2: *Initial surface with triangular mesh; (a) diagonal view, (b) plan view*

Consider a surface as shown in Fig. 2 discretized into triangular mesh. Let J_i denote the set of indices of the triangles containing vertex i. The set of indices of vertices adjacent to vertex i is denoted by N_i. The

angle of triangle $j \in J_i$ at vertex i is denoted by θ_{ji}, and the two angles of the triangles opposite to the edge ik ($k \in N_i$) are denoted by α_{ki} and β_{ki}, respectively. Then, the Gaussian curvature K_i and the mean curvature vector $\mathbf{H}_i$ at vertex i are defined as [17, 18]

$$K_i = \frac{1}{\tilde{A}_i}\left(2\pi - \sum_{j \in J_i} \theta_{ji}\right),$$

$$\mathbf{H}_i = \frac{1}{4\tilde{A}_i} \sum_{k \in N_i} (\cot \alpha_{ki} + \cot \beta_{ki})(\mathbf{p}_i - \mathbf{p}_k) \quad (3)$$

where $\tilde{A}_i$ is the area of the Voronoi region of the polyhedral surface containing vertex i, and $\mathbf{p}_i$ and $\mathbf{p}_k$ are the position vectors of vertices i and k, respectively. The discrete mean curvature H_i is obtained as the norm of $\mathbf{H}_i$, and its sign is defined by the direction of $\mathbf{H}_i$. The unit normal vector $\mathbf{n}_i$ at vertex i is defined as

$$\mathbf{n}_i = \frac{\hat{\mathbf{n}}_j}{|\hat{\mathbf{n}}_j|}, \qquad \hat{\mathbf{n}}_i = \sum_{j \in J_i} A_i \mathbf{n}_j^{\mathrm{f}} \qquad (4)$$

where A_j and $\mathbf{n}_j^{\mathrm{f}}$ are the area and the unit normal vector of face j.

Stein et al. [16] proposed a method for generating piecewise developable discrete surfaces using the Gauss map defined by the unit normal vectors of triangular faces. However, in their method, the Gauss map is not a triangulated surface, and its area cannot be easily computed. Therefore, we use the unit normal vector at each vertex so that there exists 1-to-1 correspondence between the triangles on the primary surface and those on the derived surface. The relation between the triangles of a primary surface and the Gauss map is illustrated in Fig. 3.

Primary surface   Gauss map
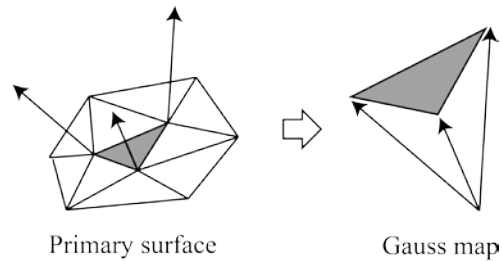
Figure 3: *Relation between the triangles of primary surface and Gauss map*

The simplest approach to generating a developable surface may be to minimize the sum of squares of Gaussian curvatures at the vertices of the primary surface. However, the square of Gaussian curvature is very insensitive to the coordinate in the normal direction of the vertex when it approaches to 0. This insensitivity may lead to a non-smooth surface shape and slow convergence of the optimization process. For example, consider a 2×2 grid with triangular mesh as shown in Fig. 4. The vertices except for the center vertex 'a' are located on the *xy*-plane, and the unit size is 1. The height (*z*-coordinate) of vertex 'a' is varied from −0.2 to 0.2, and the square of discrete Gaussian curvature at vertex 'a' and the area of the Gauss map are divided by those values at the height 0.2, respectively, to obtain the plot in Fig. 5. It is seen from the figure that the area (solid line) is more sensitive than the square of Gaussian curvature (dotted line).
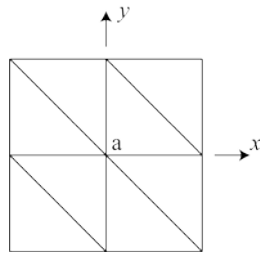

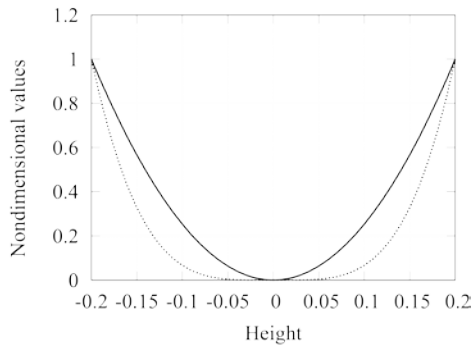**Figure 4:** *A 2×2 grid with triangular mesh.*

Figure 5: *Relation between height and nondimensional values; solid line: area of Gauss map, dotted line: square of Gaussian curvature*

In the following numerical examples, optimization is carried out using sequential quadratic programming available in SNOPT Ver. 7 [20] with the python interface of pyOpt [21]. Only *z*-coordinates of vertices are chosen as design variables.

3. SURFACE GENERATION USING GAUSS MAP

The Gauss map $c_1 = n$ is first used for generating various piecewise developable surfaces. The mean

curvature has a positive value when the surface is convex to upward, i.e., the surface in Fig. 2 has a positive mean curvature.
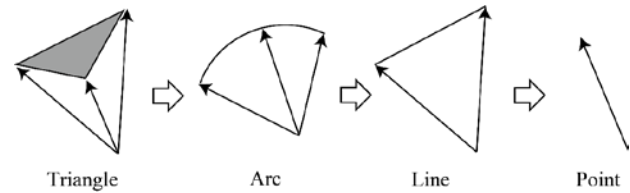

Figure 6: *Triangular face and degenerated arc, line, and point of Gauss map*
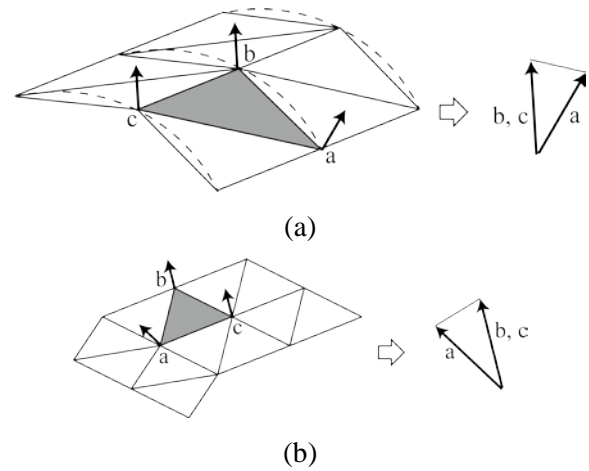

(a)

(b)

Figure 7: *Illustration of discretized developable surfaces; (a) cylindrical surface, (b) piecewise planar surface*

When the primary surface is a cylinder, the Gauss map of a triangle degenerates to an arc as shown in Fig. 6. The Gauss map may become a line if two vertices are on the same ruling (director line) as shown in Fig. 7(a). A line is generated also when a single vertex of a triangle is on the ruling, and the remaining two are on a plane that includes the ruling. This way, a cylindrical surface with the hinges in the mesh lines as well as a piecewise planar surface may be generated, as shown in Figs. 7(a) and (b), respectively, by minimizing the area of the Gauss map. Obviously, the Gauss map of a plane degenerates to a point which has zero area.

If the surface consists of three planes as shown in Fig. 8, the Gauss map of each triangle vanishes except the triangles containing vertex 'a', where three planes intersect. However, this does not have much effect if the mesh is fine enough. By contrast, if the face normal is used, the unit normal vectors of the faces in three planes, illustrated by the arrows in Fig. 8, cannot be coplanar, and the triangles should

be classified into three regions *a priori*, or classified approximately by minimizing an energy function as proposed by Stein et al. [16]. However, the face normal vectors become coplanar with vanishing area of Gauss map even when the surface has a corrugated shape with a spike as shown in the left figure of Fig. 9. This situation can be detected as a non-zero area of Gauss map if the vertex normal is used as illustrated in the right figure of Fig. 9.
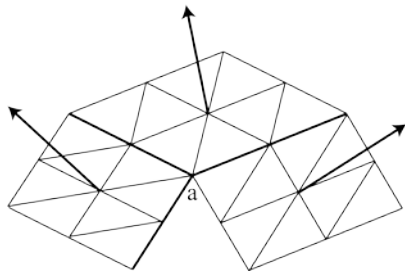

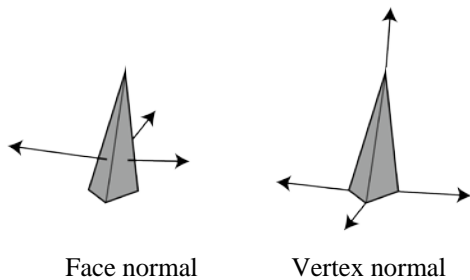**Figure 8:** *Developable surface composed of three planes*

Face normal   Vertex normal

Figure 9: *Face normal and vertex normal of a spike*
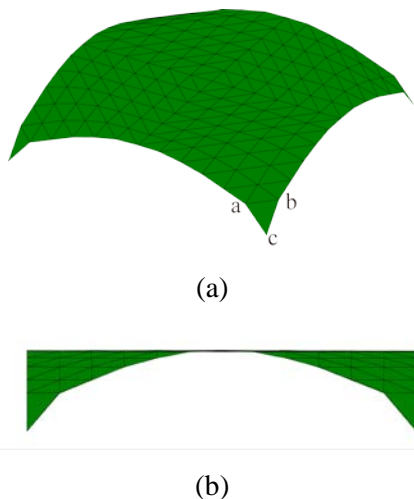

(a)

(b)

Figure 10: *Optimal shape for fixed four corners;
(a) diagonal view, (b) elevation*

The optimal surface is found from the initial triangulated surface in Fig. 2, which is a sphere with the span of 10 m and the center height of 2.929 m.

The locations of the four corners are fixed. The optimal surface minimizing the area of the Gauss map $c_1 = n$ is shown in Fig. 10. The surface has a plane around the center and cylindrical surfaces between the plane and the four corners. Hence, the surface is a piecewise developable surface. The objective function value decreases from 0.7244 to 0.0064, which is small enough, after optimization is terminated. Although the surface is distorted near the corners, the unit normal vectors at vertices 'a' and 'b' are the same, and the Gauss map of the triangle 'acb' degenerates to a line, for which the area vanishes.

It should be noted here that the surface shape with fixed four corners cannot be determined only by the vanishing area of the Gauss map, i.e., the solution to the minimization problem is non-unique. Utilizing this non-uniqueness property, various shapes of piecewise developable surfaces are generated below. However, convergence of optimization process using a nonlinear programming approach deteriorates due to the non-uniqueness of the solution. Therefore, we specify the height of the center of surface at the initial value to add restriction to the solution; i.e., the *z*-coordinate of the center vertex is excluded from the variables. The obtained shape is shown in Fig. 11. However, as seen in the figure a large distortion exists at the edges near the corner.
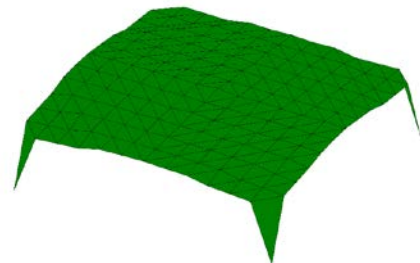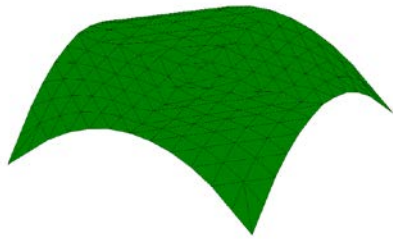

Figure 11: *Optimal shape for fixed four corners and specified height*

Although the above distortion does not lead to violation of the condition for the piecewise developable surface, it is not preferable to have a concentrated discontinuity of the normal direction near the corners. To prevent this situation, the mesh has been modified by reversing the connectivity of the (two) elements near the corner to obtain a surface as shown in Fig. 12. Although the plane around the center is slightly corrugated, a surface as a combination of a plane and four cylinders has been generated as observed from the arrows representing the gradients of triangular faces in Fig. 12(c).

97

(a)

(b)
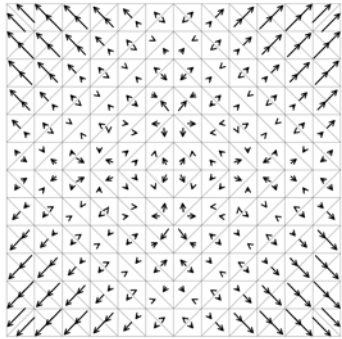
(c)

Figure 12: *Optimal shape for fixed four corners and specified height with modified mesh at corners; (a) diagonal view, (b) elevation. (c) gradients*

Although a triangle of the Gauss map degenerates to an arc with vanishing area if the primary surface is a cylinder, the difference between the cylinder and a plane can be detected by computing the side area of the triangular pyramid of the Gauss map illustrated in Fig. 3. Therefore, a plane is obtained, as shown in Fig. 13, by minimizing the sum of side areas of the triangular pyramids, although convergence is not achieved near the corner.
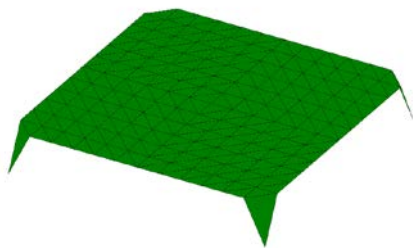
Figure 13: *Optimal shape for fixed four corners minimizing the side area*
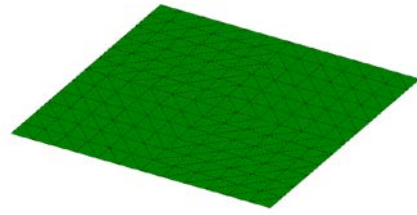
Figure 14: *Optimal shape for fixed four corners minimizing the edge length*
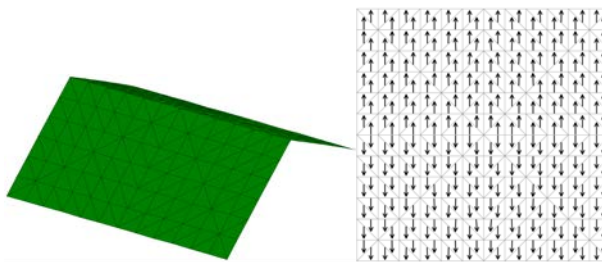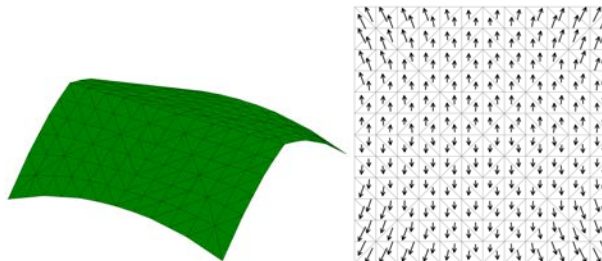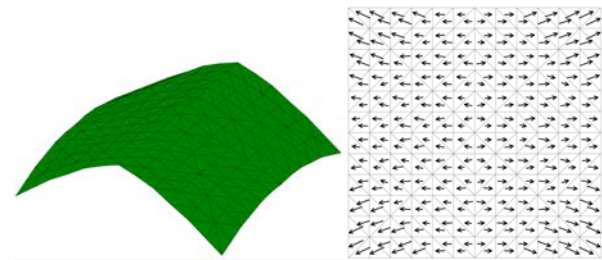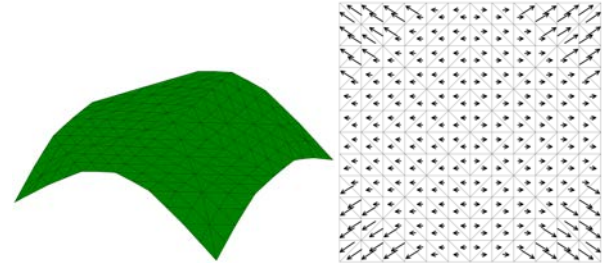
Figure 15: *Optimal shapes for fixed four corners with various internal boundaries of piecewise developable surface; left: diagonal view, right: gradients*

An arc and a point of the Gauss map can be distinguished also by computing the edge length of the triangle of the Gauss map. A plane as shown in

Fig. 14 is obtained by minimizing the sum of the edge lengths of the triangles of the Gauss map.

Next, the connectivity of the elements located along the diagonals in plan view is reversed, and the symmetry conditions are considered with respect to *xz*- and *yz*-planes. The height of the surface is fixed, and the area of the Gauss map is minimized. Let z_{i0} denote the *z*-coordinate of the *i*th vertex of the surface in Fig. 2. The initial solutions are randomly generated by a uniform distribution in the range $[z_{i0} - 0.5, z_{i0} + 0.5]$. Since the optimal solutions are non-unique, piecewise developable surfaces with various internal boundaries as shown in Fig. 15 have been obtained from different initial solutions.

The two boundaries AB and CD in the opposite sides of the initial shape in Fig. 2 are fixed at the arch shape and the other two boundaries BC and AD are modified to straight lines on the *xy*-plane as shown in Fig. 16(a). Then, a cylindrical shape as shown in Fig. 16(b) is obtained by minimizing the area of the Gauss map.
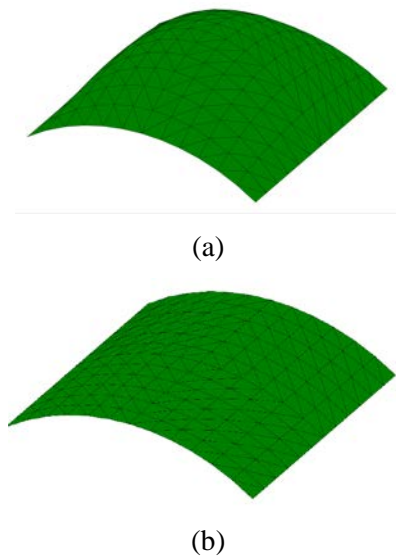
(a)

(b)

Figure 16: *Optimal shapes for fixed arch boundaries;*
(a) initial shape, (b) final shape

4. SURFACE GENERATION USING GENERALIZED OFFSET SURFACES AND GAUSS MAP

Rourier and Rando [8] proposed the area of the surface $\mathbf{c}_2 = (K + H^2)\mathbf{n}$ as a rolling metric that is minimized to generate a cylindrical surface that can be rolled. The Gauss curvature K and the mean curvature H can be computed at the internal vertices,

the area of the derived surface, which is generalized form of Gauss map, is computed only for the triangles that do not contain the boundary vertices. The surface obtained from the initial surface in Fig. 16(a) is shown in Fig. 17, which is an assembly of two cone-shaped surface.
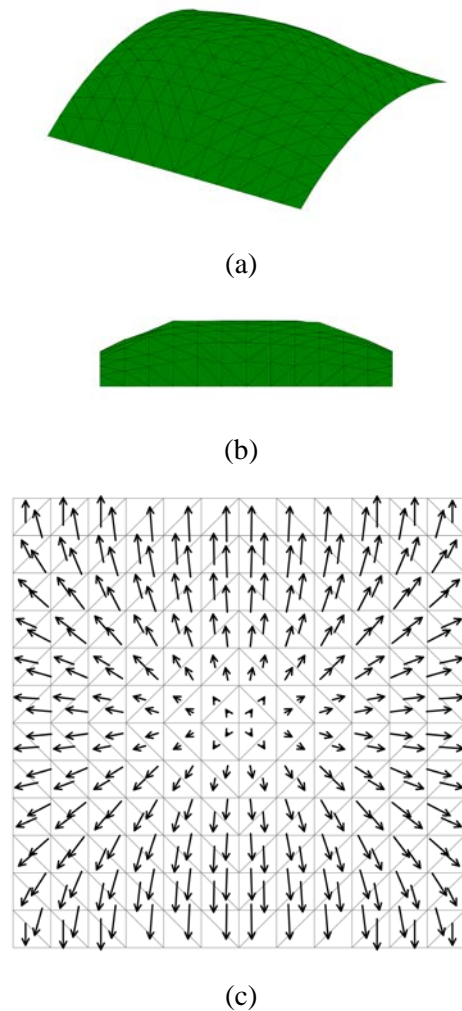
(a)

(b)

(c)

Figure 17: *Optimal shape for minimizing the area of* $\mathbf{c}_3 = (K + H^2)\mathbf{n}$ *; (a) diagonal view, (b) elevation.* *(c) gradients*

Next, we minimize the area of offset surface $\mathbf{c}_3 = \mathbf{p} - a\mathbf{n}$. If the primary surface is a sphere with the radius a, then $\mathbf{c}_3$ degenerates to the center of the sphere and its area is 0. Therefore, a round surface is to be generated by minimizing the area of $\mathbf{c}_3$. Since the span of the surface is 10 m, $a = 6$ m is chosen for the spherical shell to have an appropriate elevation at the center for the given dimensions of the shell. Only the internal vertices of the primary surface are used for generating the offset surface. From the initial surface in Fig. 2, where the four

99

corners are fixed. the optimal shape as shown in Fig. 18(a) is obtained. The surface has a round shape except near the four corners. The distortion at corner is diminished as shown in Fig. 18(b) by modifying the mesh at the corners.


(a)

(b)
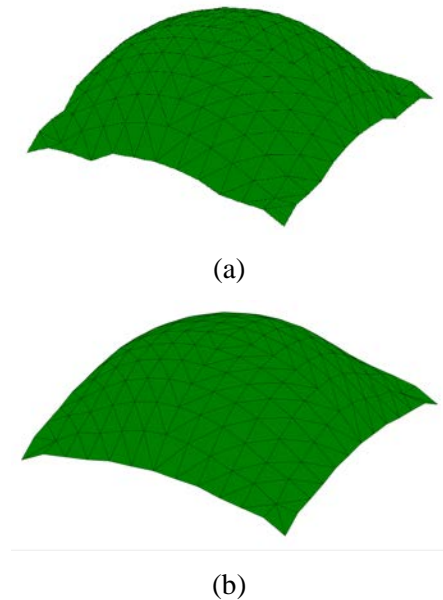
Figure 18: Optimal shapes for minimizing the area of offset surface $\mathbf{c}_3 = \mathbf{p} - a\mathbf{n}$; (a) original mesh, (b) modified mesh at corners

Finally, we minimize the area of the generalized offset surface $\mathbf{c}_4 = \mathbf{p} - (H/K)\mathbf{n}$, which is proposed as a roundness metric in Ref. [8] for obtaining a round surface close to a sphere. The obtained surface using only the internal vertices is shown in Fig. 19, which is smooth enough; however, the height becomes very large, and the triangles at the corners are distorted.
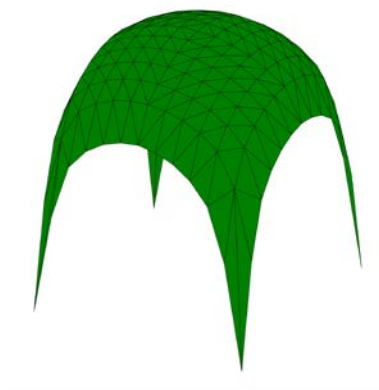
Figure 19: Optimal shapes for minimizing the area of offset surface $\mathbf{c}_4 = \mathbf{p} - (H/K)\mathbf{n}$

5. CONCLUSION

A method has been proposed for generating piecewise smooth shapes of free-form shells discretized into triangular mesh, utilizing the definitions of geometric invariants in discrete differential geometry. The discretized forms of the normal vector, Gaussian curvature, and mean curvature are used for computing the fairness measures of the surface, which are defined as the areas of derived surfaces including the generalized forms of offset surface and Gauss map.

The unit normal vectors at vertices, instead of the faces, are used for generating the derived surfaces. This way, the area of Gauss map vanishes along the internal boundaries (seam lines), and a piecewise developable surface is naturally generated by minimizing the area of the Gauss map. Non-uniqueness of the solution can be utilized to generated various shapes of piecewise developable surfaces through optimization from randomly generated initial solutions. The side area of the triangular pyramid and the edge length of the triangle of the Gauss map can also be used for the definition of the objective function to be minimized.

A round surface can be generated by minimizing the area of the offset surface with the constant distance from the primary surface; i.e., a sphere can be generated by minimizing the area of the surface that is regarded as the center of curvature of the surface. A round surface can also be generated by minimizing the roundness metric proposed in Ref. [8].

REFERENCES

[1] E. Ramm, K.-U Bletzinger and R. Reitinger, "Shape optimization of shell structures," *Bulletin of the International Association for Shell and Spatial Structures*, Vol. 34(2), pp. 103-121, 1993. (DOI: 10.1080/12506559.1993.10511083)

[2] G. Farin, *Curves and Surfaces for CAGD: A Practical Guide.* San Francisco: Morgan Kaufmann, 2001.

[3] J. Cui and M. Ohsaki, "Shape design of curved surface of membrane structure using developable surface," *Journal of the*

International Association for Shell and Spatial Structures, Vol. 59(3), pp. 199-214, September 2018.
(DOI: 10.20898/j.iass.2018.197.005)

[4]   K. Nakamura, M. Ohsaki and J. Cui, "Shape optimization of free-form shells consisting of developable surfaces," in *Spatial Structures in the 21st Century: Proceedings of the IASS Annual Symposium 2016, Tokyo, Japan, September 26-30, 2016*, K. Kawaguchi, M. Ohsaki and T. Takeuchi, Eds. 2016. Paper No. CS2E-1057.

[5]   G. Aumann, "A simple algorithm for designing developable Bézier surfaces,". *Computer Aided Geometric Design*, Vol. 20, pp. 601-619, November 2003. (DOI: 10.1016/j.cagd.2003.07.001)

[6]   K. Bandara and F. Cirak, "Isogeometric shape optimization of shell structures using multiresolution subdivision surfaces," *Computer-Aided Design*, Vol. 95, pp. 62-71, February 2018.
(DOI: 10.1016/j.cad.2017.09.006)

[7]   A. L. Bobenko, *Advances in Discrete Differential Geometry*. Berlin, Heidelberg: Springer, 2016. (DOI: 10.1007/978-3-662-50447-5)

[8]   J. A. Roulier and T. Rando, "Measures of fairness for curves and surfaces," in: *Designing Fair Curves and Surfaces: Shape Quality in Geometric Modeling and Computer-Aided Design*, N. S. Sapidis Ed., Philadelphia: SIAM, pp. 75-122, 1994. (DOI: 10.1137/1.9781611971521.ch5)

[9]   M. Ohsaki and M. Hayashi, "Fairness metrics for shape optimization of ribbed shells," *Journal of the International Association for Shell and Spatial Structures*, Vol. 41(1), pp. 31-39, April 2000.

[10] S. Fujita and M. Ohsaki, "Shape optimization of free-form shells using invariants of parametric surface," *International Journal of Space Structures*, Vol. 25(3), pp. 143-157, September 2010. (DOI: 10.1260/0266-3511.25.3.143)

[11] R. Mesnil, C. Douthe, O. Baverel and B. Léger, "Marionette Meshes: Modelling free-form architecture with planar facets,"

International Journal of Space Structures, Vol. 32(3–4), pp. 184-198, November 2017. (DOI: 10.1177/0266351117738379)

[12] U. Pinkall and K. Polthier, "Computing discrete minimal surfaces and their conjugates," *Experimental Mathematics*, Vol. 2(1), pp. 15-36, 1993.
 (DOI: 10.1080/10586458.1993.10504266)

[13] K. Hayashi, Y. Jikumaru, M. Ohsaki, T. Kagaya and Y. Yokosuka, "Discrete Gaussian curvature flow for piecewise constant Gaussian curvature surface," *Computer-Aided Design*, accepted for publication.

[14] A. Gálvez, A. Martínez and F. Milán, "Linear Weingarten surfaces in R3," *Monatshefte für Mathematik*, Vol. 138, pp. 133-144, February 2003. (DOI: 10.1007/s00605-002-0510-3)

[15] M. Shimoda and K. Yamane, "A free-form optimization method for form-finding of membrane structure," Transaction of JSME, Ser. C, Vol. 79(807), pp. 352-366, 2013. (DOI: 10.1299/kikaic.79.4353)

[16] O. Stein, E. Grinspun and K. Crane, "Developability of triangle meshes," *ACM Transactions on Graphics*, Vol. 37(4), Article 77, July 2018.
(DOI: 10.1145/3197517.3201303)

[17] J. M. Sullivan, "Curvature measures for discrete surfaces," in *SIGGRAPH 2006: ACM SIGGRAPH 2006 Courses, 2006, Boston, USA, July 30 - August 3, 2006*, J. W. Finnegan and D. Shreiner Eds. Association for Computing Machinery, 2006. pp. 10-13. (DOI: 10.1145/1185657.1185661)

[18] M. Meyer, M. Desbrun, P, Schröder and A. H. Barr, "Discrete differential-geometry operators for triangulated 2-manifolds," *Visualization and Mathematics III*. Berlin: Springer, 2003, pp. 34-47. (DOI: 10.1007/978-3-662-05105-4_2)

[19] P. E. Gill, W. Murray and M. A. Saunders, " SNOPT: An SQP algorithm for large-scale constrained optimization," *SIAM Journal on Optimization*, Vol. 12, pp. 979-1006, 2002. (DOI: 10.1137/S1052623499350013)

[20] pyOpt Documentation, Release 1.2, http://www.pyopt.org/